

University of Groningen

## Subventricular Zone Involvement Characterized by Diffusion Tensor Imaging in Glioblastoma

van Dijken, Bart Rj; Yan, Jiun-Lin; Boonzaier, Natalie R; Li, Chao; van Laar, Peter Jan; van der Hoorn, Anouk; Price, Stephen J

*Published in:*  
World neurosurgery

*DOI:*  
[10.1016/j.wneu.2017.06.075](https://doi.org/10.1016/j.wneu.2017.06.075)

**IMPORTANT NOTE: You are advised to consult the publisher's version (publisher's PDF) if you wish to cite from it. Please check the document version below.**

*Document Version*  
Final author's version (accepted by publisher, after peer review)

*Publication date:*  
2017

[Link to publication in University of Groningen/UMCG research database](#)

*Citation for published version (APA):*

van Dijken, B. R., Yan, J-L., Boonzaier, N. R., Li, C., van Laar, P. J., van der Hoorn, A., & Price, S. J. (2017). Subventricular Zone Involvement Characterized by Diffusion Tensor Imaging in Glioblastoma. *World neurosurgery*, 105, 697-701. <https://doi.org/10.1016/j.wneu.2017.06.075>

**Copyright**

Other than for strictly personal use, it is not permitted to download or to forward/distribute the text or part of it without the consent of the author(s) and/or copyright holder(s), unless the work is under an open content license (like Creative Commons).

**Take-down policy**

If you believe that this document breaches copyright please contact us providing details, and we will remove access to the work immediately and investigate your claim.

*Downloaded from the University of Groningen/UMCG research database (Pure): <http://www.rug.nl/research/portal>. For technical reasons the number of authors shown on this cover page is limited to 10 maximum.*

# Subventricular zone involvement characterised by DTI in glioblastoma

Bart RJ van Dijken BSc<sup>a,b</sup>, Jiun-Lin Yan MD<sup>a,c,d,e</sup>, Natalie R Boonzaier PhD<sup>a,c</sup>, Chao Li  
MD<sup>a,c</sup>, Peter Jan van Laar<sup>b,f</sup>, Anouk van der Hoorn MD PhD<sup>a,b,f</sup>, Stephen J Price BSc MBBS  
PhD FRCS<sup>a,c</sup>

<sup>a</sup>Brain Tumour Imaging Laboratory, Division of Neurosurgery, Department of Clinical Neuroscience, University of Cambridge, Addenbrooke's Hospital, Cambridge, UK

<sup>b</sup>Department of Radiology (EB44), University Medical Center Groningen, University of Groningen, Groningen, the Netherlands

<sup>c</sup>Wolfson Brain Imaging Centre, Department of Clinical Neuroscience, University of Cambridge, Cambridge, UK

<sup>d</sup>Department of Neurosurgery, Chang Gung Memorial Hospital, Keelung, Taiwan

<sup>e</sup>Chang Gung University College of Medicine, Taoyuan, Taiwan

<sup>f</sup>University of Groningen, University Medical Center Groningen, Center for Medical Imaging-North East Netherlands, Groningen, The Netherlands

Department of Radiology (EB44)

University Medical Center Groningen

Hanzeplein 1

P.O. Box 30.001

9700 RB Groningen, the Netherlands

*Correspondence to:*

Bart R.J. van Dijken

Telephone: +31 50 361 2400

Fax: +31 50 361 1707

[b.r.j.van.dijken@student.rug.nl](mailto:b.r.j.van.dijken@student.rug.nl)

## **KEY WORDS**

Diffusion tensor imaging

Glioblastoma

Magnetic Resonance Imaging

Neural stem cells

Subventricular zone

## **ABBREVIATIONS**

DTI – Diffusion tensor imaging

FA – Fractional anisotropy

FLIRT - FMRIB linear image registration tool

FMRIB – Functional MRI of the brain

FSL – FMRIB software library

GBM – Glioblastoma

NAWM – Normal appearing white matter

P – DTI derived isotropic component

Q – DTI derived anisotropic component

SVZ – Subventricular zone

## **ABSTRACT**

**BACKGROUND:** Glioblastomas have a poor prognosis, possibly due to a subpopulation of therapy resistant stem cells within the heterogeneous glioblastoma. As the subventricular zone is the main source of neural stem cells, we aimed at characterising the subventricular zone using DTI to demonstrate subventricular zone involvement in glioblastoma.

**METHODS:** We prospectively included 93 patients with primary glioblastomas who underwent preoperative DTI. The non-enhancing high FLAIR signal was used to describe the infiltrative tumour margin. We used a 5 mm margin surrounding the lateral ventricles to define the subventricular zone. The subventricular zone with high FLAIR was compared with the subventricular zone without high FLAIR, control high FLAIR outside the subventricular zone and control contralateral normal appearing white matter. Normalised DTI parameters were calculated and compared between the different regions.

**RESULTS:** The subventricular zone with high FLAIR showed elevated isotropic  $p$  values compared to the subventricular zone without high FLAIR ( $t(126)=3.9$ ,  $p<0.001$ ) and control regions ( $t(179)=1.9$ ,  $p=0.046$ ). Anisotropic  $q$  and fractional anisotropy values were lower in regions with high FLAIR compared to the subventricular zone without high FLAIR ( $t(181)=11.6$ ,  $p<0.001$  and  $t(184)=12.4$ ,  $p<0.001$ , respectively).

**CONCLUSION:** DTI data showed that the subventricular zone is involved in glioblastoma with elevated isotropic  $p$  values in the subventricular zone with high FLAIR, indicating tumour infiltration.

## INTRODUCTION

Glioblastoma (GBM) is the most prevalent primary malignant brain tumour in adults.<sup>1</sup> It is associated with most years of life lost despite aggressive therapy consisting of maximal safe resection followed by radiotherapy and concomitant and/or adjuvant temozolomide chemotherapy.<sup>2,3</sup> GBMs are heterogeneous tumours for which local recurrence is unavoidable due to the locally invasive behaviour of these tumours.<sup>4</sup> This local recurrence might result from a subpopulation of neural stem cells within the heterogeneity of GBM that are relatively resistant to the current therapy.<sup>5</sup>

The subventricular zone (SVZ) harbours the largest population of neural stem cells in the brain.<sup>6</sup> These stem cells were found to be astrocyte precursors which could generate multipotent neurospheres *in vitro* under the influence of epidermal growth factor and fibroblast growth factor.<sup>6-9</sup> In animals these stem cells were capable of migrating away from the SVZ.<sup>6,7</sup> Furthermore, fully differentiated astrocytes are less susceptible to malignant transformation than neural stem cells.<sup>10</sup> Hence, neural stem cells from the SVZ have received increasing interest as the possible cell of origin in GBM.

Despite the importance of the SVZ in relation to tumour initiation and the local recurrence of GBM, only a small number of imaging studies have focused on the SVZ, mainly relying on conventional MRI. However, it is known that conventional MRI does not demonstrate the local invasion of GBM that is present outside the contrast enhancement.<sup>11</sup> More advanced MRI methods, such as diffusion, better represent the biological behaviour and could identify areas of tumour invasion.<sup>12,13</sup>

We have previously histologically verified that DTI can demonstrate tumour infiltration and disruption of peritumoural white matter outside the contrast enhancement in GBM.<sup>11</sup> As GBM has the tendency to infiltrate along white matter tracts, DTI can detect subtle white matter

changes by decomposing the diffusivity into a pure isotropic component (p) and a directional anisotropic component (q).<sup>14</sup> In our image-guided biopsy study we showed that infiltration by tumour cells can be identified by elevated isotropic p components due to vasogenic oedema caused by the infiltrating cells, while disruption of white matter tracts causes a reduction in anisotropic q component.<sup>11</sup>

The SVZ thus might play an important role in GBM initiation and local tumour recurrence, but its diffusion imaging characteristics remain unknown till now. We therefore aimed to characterise the SVZ using DTI to demonstrate involvement of the SVZ in GBM. We hypothesised that the presence of tumour cells within the SVZ leads to infiltration and disruption of white matter with corresponding detectable alterations on DTI.

## **MATERIALS AND METHOD**

### **Patient Population**

We prospectively recruited patients with a supratentorial primary GBM suitable for maximal resection surgery and a WHO performance scale of 0 to 1 between 2010 and 2014. All patients underwent standard therapy consisting of maximal safe surgical resection, followed by concomitant chemoradiotherapy and adjuvant chemotherapy.<sup>3</sup> All tumours that were not GBMs in the final pathology report were excluded. All patients underwent preoperative and post-operative MRI scans. The extent of resection was classified as whether there was complete or incomplete resection of the contrast enhancing tumour. Written informed consent was obtained from all participants and this study was approved by the local institutional review board (10/H0308/23).

## **MRI acquisition**

Preoperative multi-sequence MRI data acquisition was performed using a 3.0 Tesla Siemens MR Magnetron System (Siemens Healthcare, Munich, Germany) with a standard 12-channel head coil. Preoperative imaging included T1-weighted post-contrast imaging, a T2-weighted FLAIR sequence, and DTI (figure 1). Anatomical 3D T1-weighted sequence with fat suppression was acquired after the intravenous injection of 9 ml gadolinium (Gadovist, Bayer Schering Pharma, Berlin, Germany) (TR/TE/TI 2300/2.98/900 ms; flip angle 9°; field of view 256 × 240 mm; 176-208 slices; no slice gap; voxel size 1 × 1 × 1 mm). A 2D FLAIR sequence was also acquired (TR/TE/TI 7840-8420/95/2500 ms; flip angle 150°; field of view 250 × 200 mm; 25-27 slices; 1 mm slice gap; voxel size 0.78 × 0.78 × 4 mm). DTI data was obtained using a single-shot echo-planar sequence (TR/TE 8300/98 ms; flip angle 90°; field of view 192 × 192 mm; 63 slices; no slice gap; voxel size 2 × 2 × 2 mm) with multiple b-values (0, 350, 650, 1000, 1300, and 1600 s/mm<sup>2</sup>) scanned in 13 directions comparable to our previous studies.<sup>11,14</sup>

## **Data processing**

Diffusion images were processed using tools from the Oxford Centre for Functional MRI of the Brain (FMRIB) Software Library (FSL) version 5.0.0 (<http://fsl.fmrib.ox.ac.uk/fsl/fslwiki/>, Oxford, UK). DTI data was further decomposed into an isotropic (p) component and anisotropic (q) component. DTI and FLAIR images were coregistered with preoperative T1-weighted post-contrast images by a linear transformation using the FMRIB linear image registration tool (FLIRT) functions provided by FSL.

## **Regions of Interest**

We identified the SVZ as a 5 mm margin surrounding the ventricles corresponding to earlier definitions of the SVZ used by others.<sup>15-17</sup> Ventricle masks were created in GeoS (Microsoft Corporation, Redmond, Washington, USA) from the preoperative T1-weighted post-contrast images.<sup>18</sup> Non-enhancing FLAIR maps were generated from coregistered T2-FLAIR sequences in 3D slicer (<http://www.slicer.org>). Finally, a normal appearing white matter (NAWM) control was taken from the contralateral hemisphere.

We created our ROIs in Matlab (MathWorks Inc., Natick, MA) (figure 2). We thus defined four regions:

1. The SVZ region with high FLAIR.
2. The SVZ without high FLAIR
3. Control region of high FLAIR outside the SVZ.
4. The NAWM control.

### **Statistical analysis**

All collected data was statistically tested in SPSS version 22 (IBM Inc., Armonk, NY). One-way ANOVAs with Tukey post-hoc test were used to compare the ROIs as the D'Agostino-Pearson normality test for continues and the Chi-square for dichotomous data demonstrated that all ROI data were normally distributed. A two-sided *p*-value of 0.05 was used for this study.

## **RESULTS**

### **General characteristics**



Out of the 115 initially enrolled patients, 93 met the inclusion criteria and were included in this study. The remaining 22 patients were excluded as histology demonstrated a non-GBM tumour ( $N = 11$ ), or because radiological data was not accessible ( $N = 11$ ). Patients in our cohort had a mean age of 57.6 years (range: 22-74) and 75% were males. General characteristics are summarized in table 1.

### **Imaging characteristics of the SVZ**

One way ANOVA showed that all imaging parameters demonstrated differences between the regions for all MRI parameters (isotropic (p)  $F(3,365)=70.4$ ,  $p<0.001$ ; anisotropic (q)  $F(3,365)=50.2$ ,  $p<0.001$ ; fractional anisotropy (FA)  $F(3,365)=70.8$ ,  $p<0.001$  (figure 3).

Post-hoc tests for the mean isotropic (p) DTI value (figure 3A) of the SVZ with high FLAIR showed it to be significantly higher than the SVZ without high FLAIR ( $t(126)=3.9$ ,  $p<0.001$ ), the control high FLAIR ( $t(179)=1.9$ ,  $p=0.046$ ) and the control NAWM ( $t(89)=13.7$ ,  $p<0.001$ ). The SVZ without high FLAIR showed significantly higher values than the control NAWM ( $t(92)=20.4$ ,  $p<0.001$ ). The SVZ without high FLAIR and the high FLAIR control did not differ significantly from each other ( $t(136)=-1.6$ ,  $p=0.368$ ).

For the anisotropic q component (figure 3B) the SVZ with high FLAIR showed no difference with the SVZ without high FLAIR ( $t(156)=-0.7$ ,  $p=0.782$ ) on post-hoc testing. The SVZ with high FLAIR was however significantly higher than the control high FLAIR ( $t(145)=8.2$ ,  $p<0.001$ ) and control NAWM ( $t(89)=3.1$ ,  $p=0.005$ ). The SVZ without high FLAIR was also significantly higher compared to the control high FLAIR ( $t(181)=11.6$ ,  $p<0.001$ ) and control NAWM ( $t(92)=6.0$ ,  $p<0.001$ ).

Mean FA values (figure 3C) post-hoc testing for the SVZ with high FLAIR showed significantly higher values compared to the control high FLAIR ( $t(152)=-6.3$ ,  $p<0.001$ ). It was however significantly lower compared to the SVZ without high FLAIR ( $t(154)=-3.2$ ,

$p < 0.001$ ), and control NAWM ( $t(89) = -4.9$ ,  $p < 0.001$ ). The SVZ without high FLAIR was also significantly higher than the control high FLAIR ( $t(184) = 12.4$ ,  $p < 0.001$ ) but was similar compared to the control NAWM ( $t(92) = -1.6$ ,  $p = 0.674$ ).

## DISCUSSION

In this study we characterised the SVZ in relation to GBM using DTI. Our DTI data was suggestive of tumour cells infiltrating the SVZ as isotropic  $p$  values were elevated in the SVZ with high FLAIR.

Mean isotropic  $p$  values in the SVZ with high FLAIR in our study showed an increase of  $>10\%$  compared to the SVZ without high FLAIR signal. We have previously demonstrated that an increase in isotropic  $p$  of  $>10\%$  corresponds to infiltration by tumour cells.<sup>11</sup> Interestingly, the anisotropic  $q$  values were not significantly reduced within the SVZ with high FLAIR, suggesting tumour cells infiltrated, rather than disrupted, the white matter composition. This would indicate that the tumour does not originate from the SVZ but rather grows towards it.<sup>19</sup>

Only half of GBMs may be initiated by cancer stem cells, while the other half would arise from dedifferentiated mature glial cells, based on the anatomical location of the tumour according to Lim and colleagues.<sup>20</sup> Contrary to this, Berger and colleagues proposed, cells can, besides normal mitosis, undergo an asymmetrical division.<sup>21</sup> In stem cells this means that the mother stem cell divides into one self-renewing stem cell and one progenitor cell which can further differentiate. In their work the authors suggested that cancer stem cells reside in their niche, which clinically can be a silent area, while the cancer progenitor cells would migrate away from the SVZ and give rise to a tumour.<sup>21</sup> This migratory capability of stem cells is further supported by several animal studies.<sup>6,7</sup> Also in humans SVZ stem cells have

been shown to be capable of producing neuroblasts that can migrate away from the SVZ to areas of injured brain tissue.<sup>22</sup> In infarcted areas of the brain these neuroblasts subsequently differentiated into mature neurons which are involved in brain repair mechanisms after injury. These studies suggest that SVZ stem cells could migrate to more cortical areas of the brain and initiate GBM distant from the SVZ. We therefore did not correct for the anatomical location of the tumour in the current study.

As GBMs extend outside the outer enhancing ring on conventional MRI, infiltrating tumour cells can be found within the peritumoural high FLAIR signal, although this can be mixed with vasogenic oedema effects. To overcome the limitations of conventional FLAIR imaging, more advanced MRI methods can be used in combination to demonstrate the invasive margin of GBM outside the contrast enhancement. Contrary to what would be expected in the peritumoural invasive margin, the high FLAIR control in this study did not show significantly higher isotropic p values compared with the SVZ without high FLAIR. Partial volume effects of the CSF are known to elevate isotropic diffusion measures, which possibly explains this finding.<sup>23</sup> This is further supported by the found anisotropic q values, as the high FLAIR control showed significantly lower values compared to the other regions. Our high FLAIR control showed a reduction in anisotropic q value of >21%, well above the threshold of 12% we previously used to identify disruption of white matter.<sup>11,14</sup>

## **Limitations**

A limitation of this study is that the diffusion changes are not specific for tumor infiltration, but can also represent oedema. Unfortunately, histological data is not available for our current study. However, we previously histologically validated that these diffusion changes correspond to tumour infiltration.<sup>11</sup>

## **CONCLUSION**

This study is the first to characterise the SVZ in GBM using diffusion imaging. As DTI derived isotropic p values were elevated in an area of the SVZ, suggestive of tumour infiltration, we propose that the SVZ is involved in GBM.

## **ACKNOWLEDGEMENTS**

This study was funded by a National Institute of Health Clinician Scientist Fellowship (SP), the Groningen University Fund (BD), the Marco Polo fund (BD), and grants from the Chang Gung Medical Foundation and Chang Gung Memorial Hospital, Keelung, Taiwan (JY). The authors declare to have no conflicts of interest. This paper presents independent research funded by the UK National Institute for Health Research (NIHR). The views expressed are those of the author(s) and are not necessarily those of the UK National Health Service, the UK NIHR or the UK Department of Health.

## REFERENCES

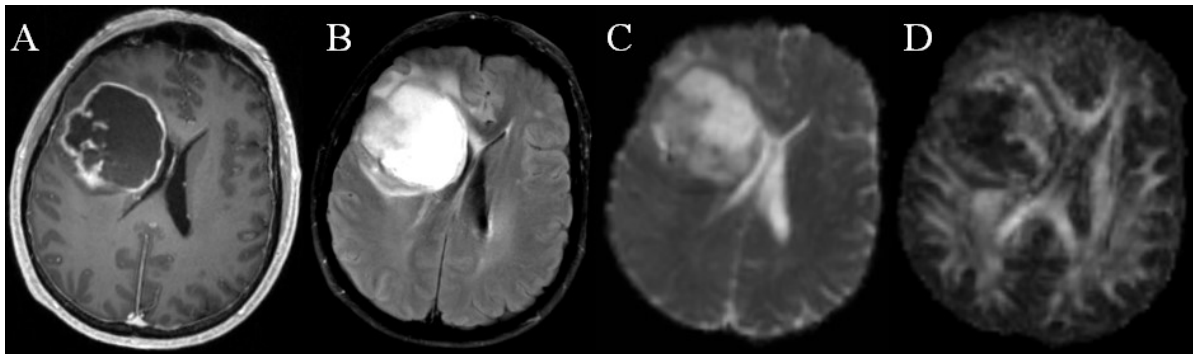
1. Ostrom QT, Gittleman H, Fulop J, et al. CBTRUS Statistical Report: Primary Brain and Central Nervous System Tumors Diagnosed in the United States in 2008–2012. *Neuro Oncol.* 2015;17:iv1-iv62.
2. Burnet NG, Jefferies SJ, Benson RJ, Hunt DP, Treasure FP. Years of life lost (YLL) from cancer is an important measure of population burden--and should be considered when allocating research funds. *Br J Cancer.* 2005;92(2):241-245.
3. Stupp R, Mason WP, Van Den Bent MJ, et al. Radiotherapy plus concomitant and adjuvant temozolomide for glioblastoma. *N Engl J Med.* 2005;352(10):987-996.
4. Sottoriva A, Spiteri I, Piccirillo SGM, et al. Intratumor heterogeneity in human glioblastoma reflects cancer evolutionary dynamics. *Proc Natl Acad Sci U S A.* 2013;110(10):4009-4014.
5. Galli R, Binda E, Orfanelli U, et al. Isolation and Characterization of Tumorigenic , Stem-like Neural Precursors from Human Glioblastoma Isolation and Characterization of Tumorigenic , Stem-like Neural Precursors from Human Glioblastoma. *Cancer Res.* 2004;64:7011-7021.
6. Sanai N, Tramontin AD, Quinones-Hinojosa A, et al. Unique astrocyte ribbon in adult human brain contains neural stem cells but lack chain migration. *Nature.* 2004;427:740-744.
7. Alvarez-Buylla A, García-Verdugo JM. Neurogenesis in adult subventricular zone. *J Neurosci.* 2002;22(3):629-634.
8. Doetsch F, Caillé I, Lim DA, García-Verdugo JM, Alvarez-Buylla A. Subventricular

- Zone Astrocytes Are Neural Stem Cells in the Adult Mammalian Brain. *Cell*. 1999;97(6):703-716.
9. Quinones-Hinojosa A, Sanai N, Soriano-Navarro M, et al. Cellular composition and cytoarchitecture of the adult human subventricular zone: A niche of neural stem cells. *J Comp Neurol*. 2006;494(3):415-434.
  10. Sanai N, Alvarez-Buylla A, Berger MS. Neural stem cells and the origin of gliomas. *N Engl J Med*. 2005;353(8):811-822.
  11. Price SJ, Jena R, Burnet NG, et al. Improved delineation of glioma margins and regions of infiltration with the use of diffusion tensor imaging: An image-guided biopsy study. *Am J Neuroradiol*. 2006;27(9):1969-1974.
  12. Verma N, Cowperthwaite MC, Burnett MG, Markey MK. Differentiating tumor recurrence from treatment necrosis: A review of neuro-oncologic imaging strategies. *Neuro Oncol*. 2013;15(5):515-534.
  13. Dhermain FG, Hau P, Lanfermann H, Jacobs AH, van den Bent MJ. Advanced MRI and PET imaging for assessment of treatment response in patients with gliomas. *Lancet Neurol*. 2010;9(9):906-920.
  14. Price SJ, Peña A, Burnet NG, et al. Tissue signature characterisation of diffusion tensor abnormalities in cerebral gliomas. *Eur Radiol*. 2004;14(10):1909-1917.
  15. Chen L, Guerrero-Cazares H, Ye X, et al. Increased Subventricular Zone Radiation Dose Correlates With Survival in Glioblastoma Patients After Gross Total Resection. *Int J Radiat Oncol Biol Phys*. 2013;86(4):616-622.
  16. Gupta T, Nair V, Paul SN, et al. Can irradiation of potential cancer stem-cell niche in

- the subventricular zone influence survival in patients with newly diagnosed glioblastoma? *J Neurooncol.* 2012;109(1):195-203.
17. Evers P, Lee PP, DeMarco J, et al. Irradiation of the potential cancer stem cell niches in the adult brain improves progression-free survival of patients with malignant glioma. *BMC Cancer.* 2010;10:384-390.
  18. Criminisi A, Sharp T, Blake A. GeoS: Geodesic image segmentation. In: *Proc. European Conference on Computer Vision (ECCV)*. Vol 5302 LNCS. ; 2008:99-112.
  19. Scherer HJ. Structural Development in Gliomas. *Am J Cancer.* 1938;34(3):333-351.
  20. Lim DA, Cha S, Mayo MC, et al. Relationship of glioblastoma multiforme to neural stem cell regions predicts invasive and multifocal tumor phenotype. *Neuro Oncol.* 2007;9(4):424-4299.
  21. Berger F, Gay E, Pelletier L, Tropel P, Wion D. Development of gliomas: Potential role of asymmetrical cell division of neural stem cells. *Lancet Oncol.* 2004;5(8):511-514.
  22. Yamashita T, Ninomiya M, Hernandez Acosta P, et al. Subventricular Zone-Derived Neuroblasts Migrate and Differentiate into Mature Neurons in the Post-Stroke Adult Striatum. *J Neurosci.* 2006;26(24):6627-6636.
  23. Chou MC, Lin YR, Huang TY, et al. FLAIR diffusion-tensor MR tractography: Comparison of fiber tracking with conventional imaging. *Am J Neuroradiol.* 2005;26(3):591-597.

## FIGURE CAPTIONS

Figure 1 – Preoperative multi-sequence MRI



Example of different MRI modalities in a patient with a large subventricular zone contacting glioblastoma: A. T1-weighted post-contrast imaging; B. T2-weighted FLAIR sequence; C. Isotropic p diffusion tensor imaging; D. Anisotropic q diffusion tensor imaging.

Figure 2 – Regions of interest

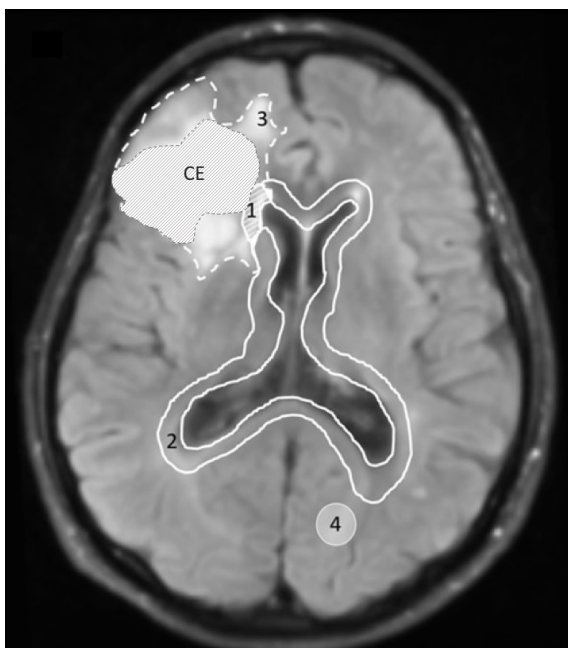
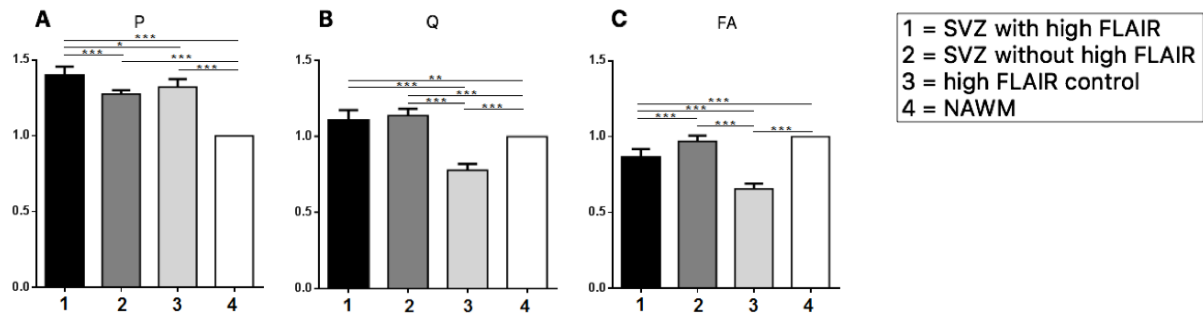


Illustration of regions of interest on an axial T2 FLAIR. 1 = Subventricular zone (SVZ) with high FLAIR; 2 = SVZ without high FLAIR; 3 = high FLAIR control; 4 = contralateral normal appearing white matter control. Abbreviations: CE = contrast enhancement;



Figure 3 – DTI characteristics in regions of interest



Normalised DTI values (A. Isotropic p; B. Anisotropic q; C. FA) in the regions of interest.

Post-hoc testing identified significant differences between the groups. Level of significance is

displayed with asterisks (\*): \* =  $p < 0.05$ ; \*\* =  $p < 0.01$ ; \*\*\* =  $p < 0.001$

Abbreviations: FA = fractional anisotropy; SVZ = subventricular zone; NAWM = normal appearing white matter.

## TABLE

Table 1 – General characteristics

Number of patients	93
Mean age (range)	57.6 (22.1–73.8)
Gender (N, %)	
- Male	70 (75.3%)
- Female	23 (24.7%)
Extent of resection (N, %)	
- Gross total	48 (51.6%)
- Subtotal	20 (21.5%)
- Biopsy	0 (0%)
- Missing	25 (26.9%)
MGMT status (N, %)	
- methylated	19 (20.4%)
- non-methylated	30 (32.3%)
- missing	44 (47.3%)
IDH-1 status (N, %)	
- mutated	5 (5.4%)
- wild-type	80 (86%)
- missing	8 (8.6%)

Abbreviations: SVZ = subventricular zone, MGMT = O6-methylguanine-DNA-methyltransferase, IDH-1 = isocitrate dehydrogenase